ChemComm

COMMUNICATION

View Article Online
View Journal | View Issue

Cite this: *Chem. Commun.*, 2019, **55**, 13450

Received 30th August 2019,
Accepted 17th October 2019

DOI: 10.1039/c9cc06767a

rsc.li/chemcomm

A succinct strategy for construction of nanoporous ionic organic networks from a pyrylium intermediate†

Siying Che,[a] Zhenzhen Yang, *[bc] Ilja Popovs,[c] Huimin Luo,[c] Yali Luo,[d] Wei Guo,[b] Hao Chen,[b] Tao Wang,[b] Kecheng Jie,[b] Congmin Wang *[a] and Sheng Dai *[bc]

Hydroxyl group and pyridinium salt-bifunctionalized nanoporous ionic organic networks prepared *via* a simple two-step strategy under metal- and template-free conditions are presented. The structural features of the resultant polymer (*e.g.* high surface area, abundant hydroxyl groups and ionic functionalities) made it a promising candidate as an efficient scavenger of toxic oxo-anions from water.

Nanoporous materials, *e.g.* activated carbons,[1] zeolites,[2] metal organic frameworks (MOFs),[3] covalent organic frameworks (COFs),[4] *etc.*, have been regarded as one of the potential candidates to meet the ever-increasing energy requirements in various systems. Among them, porous organic polymer (POP)-based species are attractive due to the easy processing and wide variability of monomers, and show typical features of high specific area, diverse pore dimensions, the use of lightweight elements only, strong covalent linkages and addressable chemical functions.[5,6] Nanoporous ionic organic networks (NIONs) are one kind of POP containing extra charges, either positive or negative, within the polymer network, as well as free counterions electrostatically bound to maintain the overall electrical neutrality.[7,8] The existence of charge on the pore wall endows the polymer skeleton with selective interactions with guest molecules due to the intrinsic charge repulsion/affinity effects. Electrostatic interactions therefore can play critical roles in amplifying separation and sorption efficiency. For the preparation of NIONs, compared with the hard/soft templating synthetic method, in which the requirement of sacrificial templates and later removal make scaled-up production difficult, direct synthesis of NIONs can be achieved by judicious choice of ionic monomers and suitable synthetic routes.[9,10] However, most of the direct synthetic approaches are conducted in the presence of metal catalysts through coupling reactions, leading to coordination of metal species with the ionic functionalities on the polymer skeletons.[11,12] Although free radical polymerization is an easy fabrication procedure of NIONs under metal-free conditions, ionic monomers with multi-vinyl groups are required and it is difficult to delicately tailor the pore structures for polymers obtained in this way.[13,14] Therefore, the development of novel and simple synthetic methodologies for the fabrication of NIONs with easy introduction of functionalities among the pore wall under metal-free conditions would propel further advancement in this field, despite still being a challenging task.

Pyrylium-based small-molecule compounds possess high oxidative power and can be easily synthesized from aldehydes and acetylbenzenes in the presence of acid, and have been utilized as a photocatalyst for promoting organic reactions under visible-light irradiation.[15,16] In addition, air and moisture stable Katritzky *N*-alkylpyridinium salts can be easily prepared from primary amines by reaction with pyrylium salts.[17] We envisaged that this simple and metal-free process could be adopted for the fabrication of NIONs with pyridinium salts within the backbone, using multi-substituted aromatic aldehydes and acetylphenyl-group containing compounds as the starting materials. This strategy also allowed introduction of other functionalities considering the abundant variability of amine structures.

In this work, a hydroxyethyl group and pyridinium salt-bifunctionalized NION (denoted as HE-Py-NION) prepared *via* a succinct two-step strategy under metal-free conditions is presented (Fig. 1). The whole process included the construction of a pyrylium-functionalized polymer through a $BF_3{\cdot}Et_2O$-catalyzed condensation reaction and subsequent transformation of the pyrylium groups into pyridium groups in the presence of amine. The introduction of additional functionality was easily realized through this approach by employing functional amines (*e.g.* ethanolamine). The resultant material HE-Py-NION possessed porous structures with a Brunauer–Emmett–Teller (BET) surface

[a] *Department of Chemistry, ZJU-NHU United R&D Center, Zhejiang University, Hangzhou 310027, China. E-mail: chewcm@zju.edu.cn*
[b] *Department of Chemistry, The University of Tennessee, Knoxville, TN, 37996, USA. E-mail: ZYANG17@utk.edu*
[c] *Chemical Sciences Division, Oak Ridge National Laboratory, P.O. Box 2008, Oak Ridge, TN 37831, USA. E-mail: dais@ornl.gov*
[d] *College of Materials Science and Engineering, Nanjing Tech University, Nanjing, 211816, P. R. China*

† Electronic supplementary information (ESI) available: Synthetic procedures of monomers and polymers, characterization, and adsorption of methylene blue hydrate and oxo-anions. See DOI: 10.1039/c9cc06767a

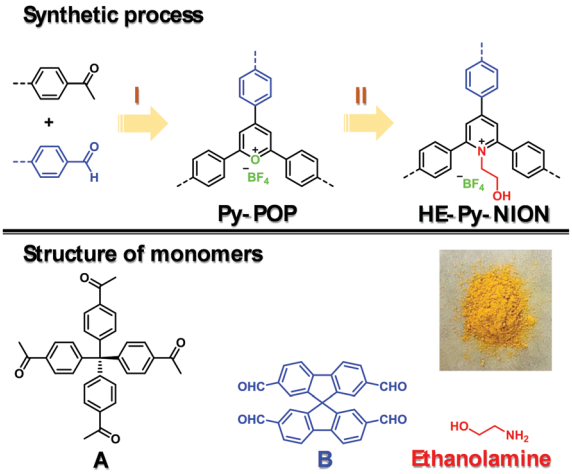

Fig. 1 Synthetic pathways of Py-POP and HE-Py-NION, and the structure of the monomers in this work; reaction conditions: step I $BF_3{\cdot}Et_2O$, 1,4-dioxane, 120 °C, 72 h; step II ethanolamine, ethanol, 100 °C, 24 h; inset: photograph of HE-Py-NION.

area of 398 $m^2\ g^{-1}$ and rapid adsorption of methylene blue hydrate owing to the existence of abundant hydroxyl groups among the backbone. The typical structural features of the polymer made it a promising candidate as an efficient scavenger of toxic oxo-anions from water.

As reported in our previous work about the fabrication of phosphabenzen-functionalized POPs,[18] pyrylium salt-containing polymers were obtained *via* a $BF_3{\cdot}Et_2O$-promoted condensation reaction in 1,4-dioxane. In this work, tetra(4-acetylphenyl)methane (A) and 9,9′-spirobi[9*H*-fluorene]-2,2′,7,7′-tetracarboxaldehyde (B) were selected as building blocks for the synthesis of pyrylium tetrafluoro borate containing POP (denoted as Py-POP) in the presence of $BF_3{\cdot}Et_2O$ (Fig. 1, step I) (for the detailed synthetic process, see the ESI†). The formation of Py-POP was verified by Fourier transformation infrared spectroscopy (FTIR), X-ray photoelectron spectroscopy (XPS), and cross-polarization magic-angle spinning (CP/MAS) ^{13}C NMR. In the FTIR spectrum of Py-POP (Fig. 2A), the characteristic bands in the range of 1400–1600 cm^{-1} belonged to the benzene rings in the skeleton and the small peak centred at 1660 cm^{-1} arose from the C═O^+ bond stretching mode in the pyrylium ring. The successful formation of the pyrylium frameworks in Py-POP was further confirmed by XPS analysis (Fig. 2B), with C, O, B and F elements observed in the survey spectra. As shown in Fig. 2C, signals for B1s with binding energy (BE) of 193.8 eV and F1s with BE of 686.9 eV corresponded to the B–F bond in the $^-BF_4$ anion. In the C1s spectrum, three peaks with BEs at 284.8, 285.8 and 289.0 eV can be deconvoluted, which were ascribed to carbons of aromatic rings/quaternary carbons, the C═O bond in terminal unreacted acetyl or aldehyde groups and C═O^+ in the pyrylium ring, respectively. The O1s spectrum also shows the presence of both a C═O^+ bond with BE of 533.7 eV and the residual unreacted C═O bond with BE of 532.0 eV. As evidenced by CP/MAS ^{13}C NMR (Fig. 2E), the formation of a pyrylium ring was confirmed by the presence of the small peak around 170.2 ppm corresponding to the carbon in the C═O^+ bond.

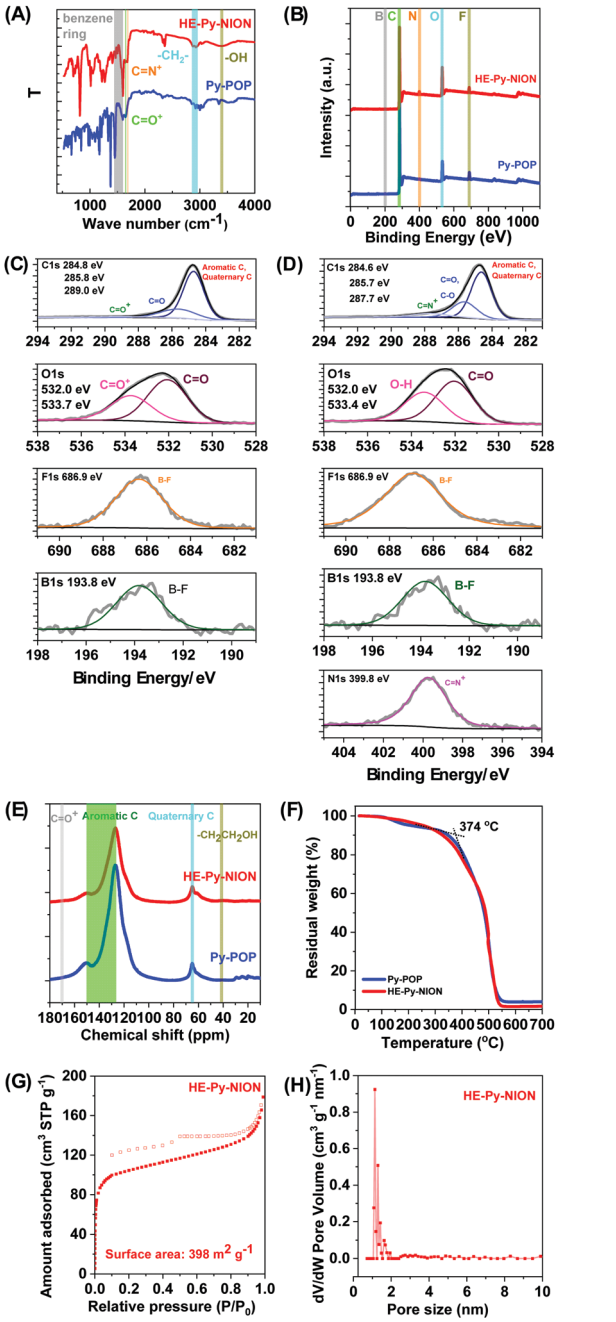

Fig. 2 Structural characterization of Py-POP and HE-Py-NION: (A) FTIR spectra. (B) XPS survey spectra. (C) C1s, O1s, F1s and B1s spectra of Py-POP. (D) C1s, O1s, F1s, B1s and N1s spectra of HE-Py-NION. (E) CP/MAS ^{13}C NMR. (F) TGA result conducted under air from 25 to 700 °C with a ramping rate of 10 °C min^{-1}. (G) N_2 sorption/desorption isotherm analysis of HE-Py-NION at 77 K. (H) Pore size distribution in HE-Py-NION.

The peaks with chemical shift in the range of 127.0–150.7 ppm belonged to the aromatic carbons in the skeleton. The peak at 64.9 ppm was attributed to the quaternary carbon. Thermogravimetric analysis (TGA) results indicated that Py-POP was stable in air up to 370 °C (Fig. 2F). The N_2 adsorption/desorption analysis result of Py-POP at 77 K (Fig. S1A, ESI†) showed that the BET surface area was 606 $m^2\ g^{-1}$ with a total

pore volume of 0.35 cm^3 g^{-1}. The pore size distribution is in the range of 0.5–2.0 nm together with a small amount of mesopores around 3.2 nm (Fig. S1B, ESI†), obtained from the adsorption branches using the non-local density functional theory (NLDFT) model.

Subsequently, Py-POP was subjected to reaction with aliphatic amine in ethanol to afford the *N*-hydroxyehtylpyridium tetrafluoro borate-functionalized NION (denoted as HE-Py-NION) in the presence of ethanolamine (Fig. 1, step II). The transformation of the pyrylium functionality to a pyridium ring is evidenced by the FTIR spectrum of HE-Py-NION (Fig. 2A), in which besides the characteristic peaks for the aromatic benzene ring in the range of 1400–1600 cm^{-1}, a new small peak appeared at 1694 cm^{-1} owing to the presence of the C=N^+ bond in the framework. The introduction of the hydroxyethyl group was confirmed by the characteristic peaks for –CH_2– units around 2914 cm^{-1} and a broad peak for –OH groups at 3400 cm^{-1}. The XPS survey spectrum of HE-Py-NION (Fig. 2B) also verified the formation of a pyridium ring, with the peak for N element being observed besides the signals for elements of B, C, O and F. As shown in Fig. 2D, in the B1s and F1s spectra, signals for B–F bonds in the BF_4^- anion almost showed no change compared with that in Py-POP. In the C1s spectrum, three peaks with BEs of 284.6, 285.7 and 287.7 eV were deconvoluted, which belonged to the aromatic ring/quaternary carbon, the C=O bond and the formed C=N^+ in the pyridium ring, respectively. The O1s spectrum also showed the presence of the –OH group with BE of 533.4 eV, together with the residual C=O bond with BE of 532.0 eV. Notably, the successful formation of pyridium units was observed in the N1s spectrum with BE of 399.8 eV for a C=N^+ bond. In the CP/MAS ^{13}C NMR spectrum of HE-Py-NION (Fig. 2E), a new small peak appeared at 40.8 ppm, indicating the introduction of a –CH_2CH_2OH group to the skeleton. The N_2 adsorption/desorption analysis result of HE-Py-NION at 77 K (Fig. 2G) showed that the BET surface area was 398 m^2 g^{-1} with a total pore volume of 0.23 cm^3 g^{-1}. The pore size distribution is in the range of 1.1–1.9 nm together with a small amount of mesopores around 3 nm (Fig. 2H). The surface area of HE-Py-NION was decreased compared with the pyrylium-functionalized polymer Py-POP, which was probably owing to the introduction of flexible hydroxyethyl groups into the skeleton. The thermal stability of HE-Py-NION was well retained compared with that of Py-POP, being stable under air up to 370 °C, as detected by TGA (Fig. 2F). According to the above results, pyridium-functionalized NION was successfully produced through a novel two-step pathway. The process was conducted under metal-free conditions, and there was no need to synthesize the ionic precursors in advance. It was easy to introduce other functional groups into the polymer backbone. Herein, hydroxyl group-containing NION was obtained by simply applying ethanolamine in the second step.

The presence of –OH groups in the skeleton of HE-Py-NION can be easily probed using a dye absorption experiment.[19] It has been reported that methylene blue hydrate (MB) dye with a nitrogen-containing aromatic ring can selectively interact with –OH groups through strong hydrogen bonding, rendering it a suitable reagent for the detection of –OH groups (Fig. 3A).[20–22]

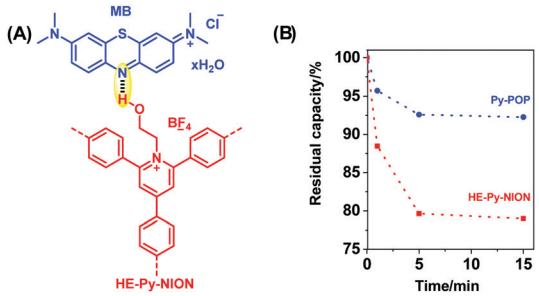

Fig. 3 (A) Hydrogen bonding between MB and HE-Py-NION. (B) Residual capacity of MB in solution as a function of time.

A faster absorption rate and greater dye adsorption was observed for HE-Py-NION compared to Py-POP (Fig. 3B), indicating that –OH groups were successfully introduced to the polymeric network of HE-Py-NION. The MB adsorption by Py-POP to some extent was probably caused by the hydrogen bonding formation between the BF_4^- anions and MB molecules. Hence, the strategy developed in this work should be an effective approach to further functionalize the pyridium NION networks by employing various aliphatic amines for task-specific applications.

To extend the application scope of the two-step methodology developed in this work, other NIONs were also fabricated. By treating Py-POP with 2,2,2-trifluoroethanamine, trifluoromethyl group and pyridinium salt-bifuntionalized NION (denoted as TFM-Py-NION) can be easily obtained with a surface area of 386 m^2 g^{-1} (Scheme S1 and Fig. S2 (ESI†)). The structure of Py-POP could also be easily changed by choosing the corresponding functionality-containing aldehydes. Besides fluorinated aldehydes previously reported by our group,[18] hydroxyl group-functionalized aldehyde was also applicable for the construction of hydroxyl group-containing Py-POP (OH-Py-POP) with a surface area of 212 m^2 g^{-1} (Scheme S2 and Fig. S3, ESI†), which can be used then for the preparation of pyridinium salt-containing NIONs by treating with amines.

Increasing water pollution caused by metal derived oxo-anions (CrO_4^{2-}, TcO_4^-, SeO_3^{2-}, AsO_4^{3-}, *etc.*) has drawn much attention worldwide,[23] and these oxo-anions have been included in the priority pollutant list by the EPA (Environmental Protection Agency, U.S.).[24] Until now, various techniques have been developed for removal of oxo-anions including ion exchange, chemical precipitation, adsorption, electrodialysis, photocatalysis and so on, among which an ion exchange method showed the advantages of being low cost, comparatively simple and safe, and efficient performance.[25] In this respect, materials such as anion exchange resins, layered double hydroxides (LDHs), and cationic metal–organic frameworks (MOFs) have been developed.[26–28] However, anion exchange resins had drawbacks of poor exchange kinetics and lack of stability. Although MOFs have been employed to capture oxo-anions from water, lack of sufficient physiochemical stability and difficulties in the bulk scale synthesis have hindered their wide application.[29] In contrast, porous organic materials, especially NIONs, are constructed from strong covalent bonds, leading to high physiochemical stability, which made them promising candidates in oxo-anion capture.[9,12,30]

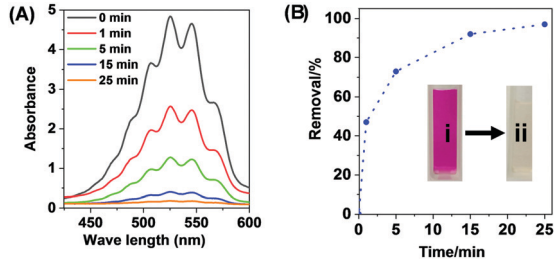

Fig. 4 (A) UV-Vis spectroscopy in the presence of HE-Py-NION for the water solution of MnO_4^-. (B) Removal (in %) of MnO_4^- ions at different time intervals. Inset: Photograph of (i) the starting MnO_4^- solution and (ii) the MnO_4^- solution in the presence of HE-Py-NION after 25 min.

Recently, Ghosh *et al.* has reported the application of a viologen-based cationic organic network in the capture of hazardous anionic pollutants from water with high capacity.[30]

Herein, MnO_4^- was taken as a model ion, which is a close chemical analogue of TcO_4^- and ReO_4^- (Mn, Tc and Re belonged to the same group in the periodic table). The MnO_4^- capture study was monitored at 525 nm (λ_{max}) (for experimental details, see the ESI†). In the previous study using an ionic viologen-organic network as a scavenger,[30] 0.5 mM solution of MnO_4^- was adopted and almost complete removal was observed within 5 min. However, when the performance of HE-Py-NION in MnO_4^- capture was measured first under the same conditions (0.5 mM MnO_4^- 2 mL and HE-Py-NION 1 mg), pretty rapid adsorption was observed within a few seconds. Comparatively, almost no MnO_4^- absorption was observed in the presence of Py-POP under the otherwise identical conditions (Fig. S4, ESI†), probably owing to the hydrophobic nature and hence poor dispersity of Py-POP in aqueous solution. Therefore, the introduction of hydroxyl groups within the backbone could render good dispersity of the polymer in aqueous solutions. In order to make the process measurable, a higher MnO_4^- concentration of 5 mM was used instead and the result is shown in Fig. 4. A rapid decrease in the absorption spectra was observed and within 25 min the solution got decolorized from purple, indicating the complete removal. A maximum adsorption capacity of 1.145 g g^{-1} could be achieved for $KMnO_4$ by HE-PyNION, exceeding that of the Ionic viologen-organic network (0.297 g g^{-1})[30] and the Cu(I)-based cationic MOF (SLUG-21) (0.283 g g^{-1}).[24] We proposed that the synergistic effect of abundant anionic and hydroxyl functionalities in the polymer backbone as well as the high surface area of HE-Py-NION played a crucial role in achieving the superior oxo-anion removal performance seen in these systems.

In summary, a novel two-step synthetic pathway was developed for the preparation of hydroxyl-group functionalized porous ionic polymers. The synthesis was conducted under metal-free conditions and without the need for the synthesis of ionic pair-containing monomers. Notably, this is also a straightforward way to induce other functional groups into the ionic skeleton simply by employing various amines. The resultant polymer HE-Py-NION showed rapid adsorption of MB owing to the existence of abundant hydroxyl groups among the backbone. The structural characterization of the polymer also made it a promising candidate as an efficient scavenger of toxic oxo-anions from water.

This research was supported financially by the Division of Chemical Sciences, Geosciences, and Biosciences, Office of Basic Energy Sciences, US Department of Energy.

Conflicts of interest

There are no conflicts to declare.

References

1 M. R. Benzigar, S. N. Talapaneni, S. Joseph, K. Ramadass, G. Singh, J. Scaranto, U. Ravon, K. Al-Bahily and A. Vinu, *Chem. Soc. Rev.*, 2018, **47**, 2680–2721.
2 M. Shamzhy, M. Opanasenko, P. Concepción and A. Martínez, *Chem. Soc. Rev.*, 2019, **48**, 1095–1149.
3 M. Zhao, Y. Huang, Y. Peng, Z. Huang, Q. Ma and H. Zhang, *Chem. Soc. Rev.*, 2018, **47**, 6267–6295.
4 S. Kandambeth, K. Dey and R. Banerjee, *J. Am. Chem. Soc.*, 2019, **141**, 1807–1822.
5 J. Wu, F. Xu, S. Li, P. Ma, X. Zhang, Q. Liu, R. Fu and D. Wu, *Adv. Mater.*, 2019, **31**, 1802922.
6 X.-Y. Yang, L.-H. Chen, Y. Li, J. C. Rooke, C. Sanchez and B.-L. Su, *Chem. Soc. Rev.*, 2017, **46**, 481–558.
7 J.-K. Sun, M. Antonietti and J. Yuan, *Chem. Soc. Rev.*, 2016, **45**, 6627–6656.
8 S. Zhang, K. Dokko and M. Watanabe, *Chem. Sci.*, 2015, **6**, 3684–3691.
9 P. Zhang, Z.-A. Qiao, X. Jiang, G. M. Veith and S. Dai, *Nano Lett.*, 2015, **15**, 823–828.
10 C. Gao, G. Chen, X. Wang, J. Li, Y. Zhou and J. Wang, *Chem. Commun.*, 2015, **51**, 4969–4972.
11 Y. Tian, J. Song, Y. Zhu, H. Zhao, F. Muhammad, T. Ma, M. Chen and G. Zhu, *Chem. Sci.*, 2019, **10**, 606–613.
12 O. Buyukcakir, S. H. Je, D. S. Choi, S. N. Talapaneni, Y. Seo, Y. Jung, K. Polychronopoulou and A. Coskun, *Chem. Commun.*, 2016, **52**, 934–937.
13 Q. Sun, Y. Jin, B. Aguila, X. Meng, S. Ma and F.-S. Xiao, *ChemSusChem*, 2016, **10**, 1160–1165.
14 X. Wang, Y. Zhou, Z. Guo, G. Chen, J. Li, Y. Shi, Y. Liu and J. Wang, *Chem. Sci.*, 2015, **6**, 6916–6924.
15 N. J. Gesmundo and D. A. Nicewicz, *Beilstein J. Org. Chem.*, 2014, **10**, 1272–1281.
16 K. Wang, L. G. Meng and L. Wang, *Org. Lett.*, 2017, **19**, 1958–1961.
17 J. Wu, P. S. Grant, X. Li, A. Noble and V. K. Aggarwal, *Angew. Chem., Int. Ed.*, 2019, **58**, 5697–5701.
18 Z. Yang, H. Chen, B. Li, W. Guo, K. Jie, Y. Sun, D.-E. Jiang, I. Popovs and S. Dai, *Angew. Chem., Int. Ed.*, 2019, **58**, 13763–13767.
19 J. Zhang, Z.-A. Qiao, S. M. Mahurin, X. Jiang, S.-H. Chai, H. Lu, K. Nelson and S. Dai, *Angew. Chem., Int. Ed.*, 2015, **54**, 4582–4586.
20 H. Kosonen, S. Valkama, A. Nykänen, M. Toivanen, G. ten Brinke, J. Ruokolainen and O. Ikkala, *Adv. Mater.*, 2006, **18**, 201–205.
21 S. Valkama, A. Nykänen, H. Kosonen, R. Ramani, F. Tuomisto, P. Engelhardt, G. ten Brinke, O. Ikkala and J. Ruokolainen, *Adv. Funct. Mater.*, 2007, **17**, 183–190.
22 G. Ji, Z. Yang, H. Zhang, Y. Zhao, B. Yu, Z. Ma and Z. Liu, *Angew. Chem., Int. Ed.*, 2016, **55**, 9685–9689.
23 L. Keith and W. Telliard, *Environ. Sci. Technol.*, 1979, **13**, 416–423.
24 H. Fei, D. L. Rogow and S. R. J. Oliver, *J. Am. Chem. Soc.*, 2010, **132**, 7202–7209.
25 A. V. Desai, B. Manna, A. Karmakar, A. Sahu and S. K. Ghosh, *Angew. Chem., Int. Ed.*, 2016, **55**, 7811–7815.
26 L. Zhu, L. Zhang, J. Li, D. Zhang, L. Chen, D. Sheng, S. Yang, C. Xiao, J. Wang, Z. Chai, T. E. Albrecht-Schmitt and S. Wang, *Environ. Sci. Technol.*, 2017, **51**, 8606–8615.
27 X. Zhao, X. Bu, T. Wu, S.-T. Zheng, L. Wang and P. Feng, *Nat. Commun.*, 2013, **4**, 2344.
28 Y. Li, Z. Yang, Y. Wang, Z. Bai, T. Zheng, X. Dai, S. Liu, D. Gui, W. Liu, M. Chen, L. Chen, J. Diwu, L. Zhu, R. Zhou, Z. Chai, T. E. Albrecht-Schmitt and S. Wang, *Nat. Commun.*, 2017, **8**, 1354.
29 S. Keskin, T. M. van Heest and D. S. Sholl, *ChemSusChem*, 2010, **3**, 879–891.
30 P. Samanta, P. Chandra, S. Dutta, A. V. Desai and S. K. Ghosh, *Chem. Sci.*, 2018, **9**, 7874–7881.